Machinery & Energetics
Vol. 14, No. 2. 2023

Journal homepage:
https://technicalscience.com.ua/en

UDC 535.372, 628.9.037
DOI: 10.31548/machinery/2.2023.80

Volodymyr Boyko
PhD in Physical and Mathematical Sciences, Associate Professor
National University of Life and Environmental Sciences of Ukraine
03041, Heroiv Oborony st., 15, Kyiv, Ukraine
https://orcid.org/0000-0003-2926-2752

Vitalii Chornii*
PhD in Physical and Mathematical Sciences
National University of Life and Environmental Sciences of Ukraine
03041, Heroiv Oborony st., 15, Kyiv, Ukraine
https://orcid.org/0000-0003-3727-5617

Serhii Nedilko
Doctor of Physical and Mathematical Sciences, Senior Researcher
Taras Shevchenko National University of Kyiv
01601, Volodymyrska st., 64/13, Kyiv, Ukraine
https://orcid.org/0000-0001-5196-6807

Kateryna Terebilenko
Doctor of Chemistry, Associate Professor
Taras Shevchenko National University of Kyiv
01601, 64/13 Volodymyrska Str., Kyiv, Ukraine
https://orcid.org/0000-0003-2403-4347

Luminescent converters based on "nanocellulose + $K_3Tb(PO_4)_2$:Eu" composite films

Abstract. The advantages of cellulose and its derivatives as the latest materials for devices that generate, store, and convert electricity are their low cost, environmental friendliness, ease of recycling and the ability to be manufactured in various ways and from various raw materials, including agricultural waste. This predetermines the relevance of their study as materials for modern technology and electronics. The research aims to determine the luminescent characteristics of composite films made based on nanocellulose and polycrystalline oxide $K_3Tb_{0.9}Eu_{0.1}(PO_4)_2$. Optical microscopy and the spectral-luminescence method were used to characterise the films and their initial components. It was found that crystallites with an average size of about 50 μm are distributed quite evenly in the film "nanocellulose +$K_3Tb_{0.9}Eu_{0.1}(PO_4)_2$". A Raman scattering band with a maximum of 564 nm under laser excitation at 473 nm was observed for the investigated samples in the form of suspensions. The intensity of photoluminescence of nanocellulose in suspension and films is low compared to the luminescence of oxide as a filler. The luminescence of Eu^{3+} ions is intense in the red region of the spectrum. The calculated values of the degree of asymmetry indicate low symmetry of the positions occupied by europium ions in the oxide and the contribution of Tb^{3+} ion emission to the overall spectrum of the composite film. The study results show that the luminescence of Eu^{3+} ions is sensitised by Tb^{3+} ions, which absorb the excitation light and then transfer energy to europium ions. The position of the absorption bands of Eu^{3+} and Tb^{3+} ions in the ultraviolet region of the spectrum and

Article's History: Received: 13/01/2023; Revised: 07/04/2023; Accepted: 26/04/2023.

Suggested Citation:
Boyko, V., Chornii V., Nedilko, S., & Terebilenko, K. (2023). Luminescent converters based on "nanocellulose + $K_3Tb(PO_4)_2$:Eu" composite films. *Machinery & Energetics,* 14(2), 80-89. doi: 10.31548/machinery/1.2023.80.

*Corresponding author

the intense emission of Eu^{3+} in the red region indicates the prospects of using nanocellulose + $K_3Tb_{0.9}Eu_{0.1}(PO_4)_2$ films to improve the efficiency of solar panels. Testing of the films under the excitation of luminescence by ultraviolet radiation of an LED (λ_{ex} = 375 nm) showed the possibility of developing white LEDs on their basis. In particular, the chromaticity coordinates of the uncoated LED were (x = 0.214; y = 0.079), and the use of a film composite as a coating causes a shift in the coordinates to the red region: x = 0.304, y = 0.196. The obtained results on the morphology and luminescent properties can be used to optimise the composition and manufacturing conditions of composite films of the following types "nanocellulose +$K_3Tb_{0.9}Eu_{0.1}(PO_4)_2$" for use as fluorescent converters in LEDs or solar panels

Keywords: ion; sensitisation; LED; solar panel; photoluminescence; coating

INTRODUCTION

At the current stage of equipment and technology development, in particular, those related to the production, storage and conversion of electricity, a significant need for low-cost materials exists. One of the challenges is also the significant increase in waste associated with electronic devices. According to analysts V. Forti *et al*. (2020), the rate of electronics waste generation will be around 74.7 million tonnes per year by 2030. Only a small part of this waste is recycled, and the rest pollutes the environment (Ahirwar & Tripathi, 2021). Thus, the latest materials need to be cheap and easy to dispose of. There is a growing focus on cellulose as a material for modern technologies (Fang *et al.*, 2021; Zhao *et al.*, 2021). Cellulose is a fairly cheap natural polymer due to the abundance of its sources (from wood raw materials to agricultural waste) and well-developed manufacturing technologies. Nanocellulose (NC) is also being actively researched, in particular, the kind that is produced by an environmentally friendly bacterial method with minimal use of chemicals (Urbina *et al.*, 2021; Choi *et al.*, 2022). In addition to being cheap, cellulose and its derivatives are environmentally friendly, biocompatible, and naturally biodegradable. N.C. Raut & K. Al-Shamery (2018) and P. Wang *et al.* (2018) found that 3D printing technology has given an additional impetus to the development of cellulose-based materials for technology and the creation of a whole area of "paper" electronics. The study by D. Choe *et al.* (2018) and I. Indriyati *et al.* (2019) have shown that the physical and chemical properties of cellulose significantly depend on the method of manufacture and further processing. Therefore, to improve the properties of this natural polymer, impurities of a certain nature are added to it, depending on the intended use. For example, the addition of zinc, nickel, and carbon oxide nanoparticles to cellulose is proposed as a way to obtain a lightweight, flexible, and low-cost material for solar panels, as reported by G.F. Gemeda *et al.* (2022) and X. Liu *et al.* (2020). Composites based on cellulose and inorganic polymers or carbon nanostructures have been investigated as promising materials for dielectric capacitors and supercapacitors (Pal *et al.*, 2022; Wang *et al.*, 2023; Zhu *et al.*, 2023). M. Nedielko *et al.* (2018) and J. Gan *et al.* (2022) noted that microcrystalline cellulose incorporated with luminescent particles is a promising material for luminescent light converters and LEDs. For such systems, the interaction between the elements of the cellulose matrix and the filler is important. It is the presence of such interaction between the components that allows us to assert the presence of a composite material whose properties are not the "sum" of the properties of its components. Despite a significant number of scientific studies of cellulose-based composites, there is almost no understanding of the processes and ways of this interaction due to the overall complexity of the material structure, which makes this study relevant.

The research aimed to fabricate and determine the luminescent characteristics of composite films based on NC and $K_3Tb_{0.9}Eu_{0.1}(PO_4)_2$ oxide, which have prospects for use as luminescent coatings for LEDs or solar cell components. The morphology and optical properties of films of this composition have not been studied before. The optical properties of composites with luminescent oxides have been the subject of a rather limited number of scientific papers. The main research objectives were to fabricate the films, measure the photoluminescence (PL) and PL excitation spectra, and analyse the spectral characteristics from the perspective of the practical application of these luminescent materials.

MATERIALS AND METHODS

The production of the films (NC and "NC+ $K_3Tb_{0.9}Eu_{0.1}(PO_4)_2$") and the study of their morphology using optical microscopy were carried out at the Department of Physics of the National University of Life and Environmental Sciences of Ukraine in February 2023. The study of the spectral and luminescent properties of the films was carried out at the Faculty of Physics of Taras Shevchenko National University of Kyiv in March and April 2023. The choice of the composite film components was based on the following considerations: it is known that pure cellulose exhibits visible photoluminescence, the characteristics of which depend on the excitation wavelength (Nedielko *et al.*, 2017; Zou *et al.*, 2019). Thus, such a polymer matrix should play an active role in the processes of light absorption and emission in the composite. The NC consists of nanoscale structures (crystals, whiskers, fibrils) that can be easily arranged near the surface of the filler particle. In this case, the effective contact area between the oxide and the cellulose should be larger than in the case of composites based on microcrystalline cellulose, in which the filler occupies only a part of the space between the fibres. As for the choice of the oxide filler, $K_3Tb(PO_4)_2$:Eu, this material

is characterised by intense photoluminescence in the red spectral region when excited by ultraviolet (UV) radiation (Mikhailik *et al.*, 2009). Accordingly, it was expected that the manufactured nanocomposites would be capable of converting UV radiation into visible light.

Production of nanocellulose films and composites samples "NC+$K_3Tb_{0,9}Eu_{0,1}(PO_4)_2$" was carried out using a nanocellulose suspension in water (dry matter content: 0.6 wt%). The conditions for obtaining this suspension and its characteristics have been described in detail previously (Barbash *et al.*, 2019). Synthesis of oxide $K_3Tb_{0,9}Eu_{0,1}(PO_4)_2$ was made from fluoride melts using a method similar to that described in the study (Terebilenko *et al.*, 2017). The procedure for making the films was as follows: thoroughly ground oxide powder $K_3Tb_{0,9}Eu_{0,1}(PO_4)_2$ in the amount of 30 mg was mixed with 2 ml of distilled water and sonicated (f = 4.2 kHz) for 10 min. To the resulting mixture was added 3 ml of nanocellulose suspension. The resulting liquid, after "NC+$K_3Tb_{0,9}Eu_{0,1}(PO_4)_2$" ultrasound treatment for 1 hour, evaporated at 56°C for 4 hours, and then at room temperature in an open space for 2 days. The resulting gel was poured onto a glass substrate, where it was kept for another day until it dried completely to form a film. An identical procedure (except for the addition of oxide) was used to obtain a film of "pure" (without oxide) NC as a comparison sample. The film of "pure" NC was transparent, while the film with oxide was less transparent and matte.

The film samples were examined using an optical microscope and a spectral-luminescence complex consisting of a DFS-12 spectrometer (USSR) with an FEU-100 photomultiplier (USSR), a DMR-4 prism monochromator (USSR), a powerful xenon lamp DKsEL-1000 (USSR), and diode-pumped lasers (λ_{rad} = 405 and 473 nm).

RESULTS AND DISCUSSION

Figure 1 shows micrographs of samples of NC suspension, powder $K_3Tb_{0,9}Eu_{0,1}(PO_4)_2$, NC film and "NC+$K_3Tb_{0,9}Eu_{0,1}(PO_4)_2$" film obtained using an optical microscope in the light transmitted through the sample. For the initial NC suspension, a certain number of thin, long microstructures are observed, which are cellulose microfibrils (Fig. 1a). Rectangular formations, such as cellulose microcrystals, can also be seen. Figure 1b shows the area with the largest $K_3Tb_{0,9}Eu_{0,1}(PO_4)_2$ particles with a size of ~300 μm. However, the vast majority of oxide powder particles are several μm and even smaller. These small particles form small dark-coloured agglomerates, which are destroyed by ultrasound. For the thin NC film (Fig. 1c), a significant number of microcrystals is observed. In contrast to the case of the nanocellulose suspension, no microfibrils are observed here, which may be due to the destruction of the latter under the action of ultrasound. In the case of the film "NC+$K_3Tb_{0,9}Eu_{0,1}(PO_4)_2$" A fairly uniform distribution of oxide crystals without significant particle agglomerates can be observed (Fig. 1d).

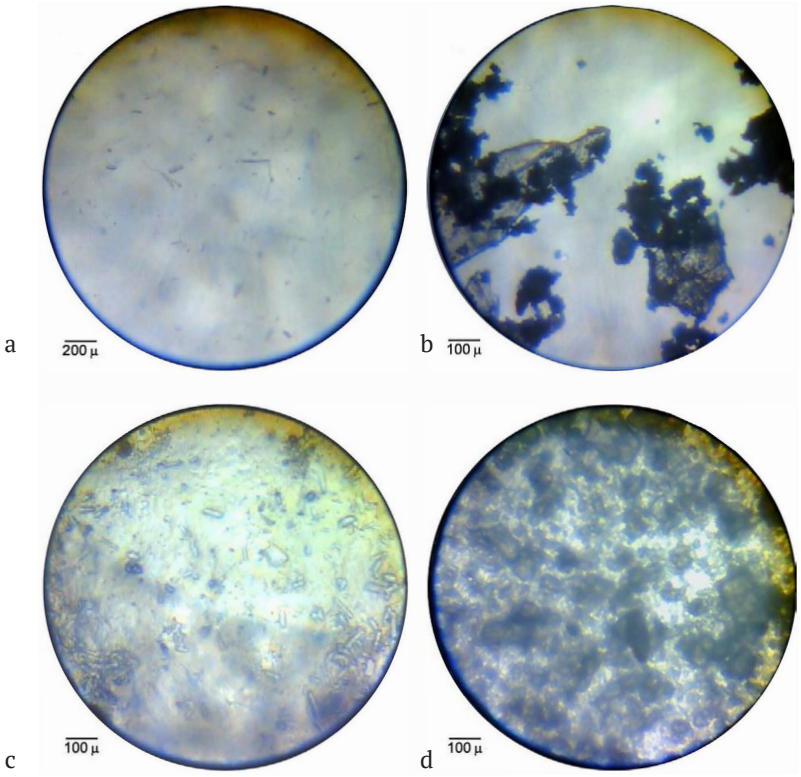

Figure 1. Microphotos
Note: a) NC suspension drop, b) powder $K_3Tb_{0.9}Eu_{0.1}(PO_4)_2$, c) NC film, d) film "NC+$K_3Tb_{0.9}Eu_{0.1}(PO_4)_2$"
Source: compiled by the authors

Figure 2 shows the photoluminescence spectra of the powder $K_3Tb_{0.9}Eu_{0.1}(PO_4)_2$, NC and "NC+$K_3Tb_{0.9}Eu_{0.1}(PO_4)_2$" suspensions. In the PL spectrum of oxide under laser excitation, (473 nm), rather narrow bands associated with the emission of Tb^{3+} (electronic transition $^5D_4 \rightarrow {}^7F_6$, λ_{max} = 543 nm) and Eu^{3+} ions (transition $^5D_0 \rightarrow {}^7F_{0\text{-}4}$: remaining lines on spectrum 1, Fig. 2) are observed. The peculiarity of the Tb^{3+} and Eu^{3+} ions is their $4f^N$ shielded electron shells, within which the above electronic transitions occur (Dorenbos, 2000). As a result of the shielding, the position of the maxima of the corresponding bands weakly depends on the immediate environment of the ions and the PL excitation conditions. Therefore, the data obtained in the present study on the luminescent properties of $K_3Tb_{0.9}Eu_{0.1}(PO_4)_2$ are consistent with the results of V.B. Mikhailik *et al*. (2009), despite the different PL excitation conditions.

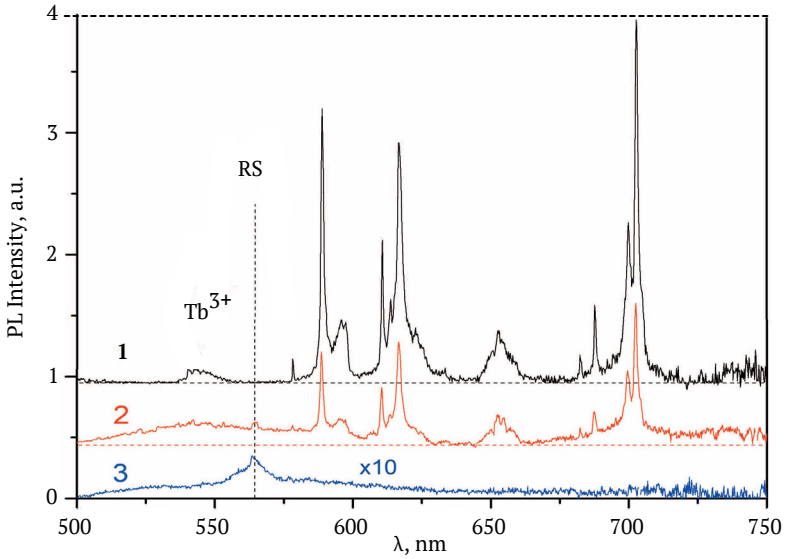

Figure 2. Photoluminescence spectra

Note: 1) powder $K_3Tb_{0.9}Eu_{0.1}(PO_4)_2$, 2) suspension "NC+ $K_3Tb_{0.9}Eu_{0.1}(PO_4)_2$", 3) initial NC suspension, λ_{enr}=473 nm, T=295 K. The zero-signal level for spectra 1 and 2 is shown by horizontal dashed lines

Source: compiled by the authors

The initial nanocellulose suspension at 473 nm excitation is characterised by a low-intensity PL (spectrum 3 in Fig. 2), which is due to the low polymer content (0.6 wt%) and the PL attenuation by water molecules. The band of this PL is very broad, and complex, and extends from 500 to 730 nm. It is quite similar to the PL of microcrystalline cellulose (Nedielko *et al.*, 2017) and is associated with a set of PL centres arising from carbonyl, carboxyl, and methyl molecular groups. Against the background of the PL band of nanocellulose, a rather narrow band with a maximum of 564 nm is observed (the position is shown by a vertical dashed line and denoted RS). This band is a manifestation of Raman scattering of laser radiation on water molecules. Indeed, taking the difference in the frequency of the band maximum position (ν≈17730 cm^{-1}) and the laser frequency (ν≈21140 cm^{-1}), a frequency of Δν≈3410 cm^{-1}, which corresponds to the stretching/compressing vibrations of OH groups in water, was obtained (Beran *et al.*, 2001).

The photoluminescence spectrum of the suspension "NC+$K_3Tb_{0.9}Eu_{0.1}(PO_4)_2$" contains both bands associated with the NCs and those related to the luminescence centres in the oxide. It is worth noting that in this experiment, a suspension was used from which 4 ml of water was evaporated. This results in a significant weakening of the Raman scattering band in the spectrum 2 Figure 2, as well as a certain increase in the intensity of the PL band of nanocellulose. Such a suspension can be used as the basis for luminescent inks for 3D printing of paper electronics elements (Zhuravlov *et al.*, 2021).

The presence of a narrow weak PL band with a maximum at 579 nm, which is associated with the transition $^5D_0 \rightarrow {}^7F_0$ in the ion of Eu^{3+}, for oxide powder $K_3Tb_{0.9}Eu_{0.1}(PO_4)_2$ and suspension "NC+$K_3Tb_{0.9}Eu_{0.1}(PO_4)_2$" (spectra 1 and 2, Fig. 2) indicates a rather low symmetry of the surroundings of this ion both in the original oxide and in the case when the oxide particles are in the NC suspension. This result is consistent with the crystallographic data (Farmer *et al.*, 2016), according to which the trivalent cation in $M_3RE(PO_4)_2$ systems, where M is an alkali metal and RE is a rare earth ion, occupies a position with the symmetry of the surroundings – C_{2v}. In the 585-600 nm region, bands of $^5D_0 \rightarrow {}^7F_1$ magneto-dipole transitions in Eu^{3+} ions are observed. A detailed examination of spectra 1 and 2 (Fig. 2) reveals 3 components in this region, which, according to K. Binnemans (2009), is evidence of low symmetry of the Eu^{3+} ion environment or the presence of two different types of emission centres.

R. Reisfeld *et al.* (2004) demonstrated that the ratio of the integrated PL intensities for the transitions $^5D_0 \rightarrow {}^7F_2$

(600-635 nm) and $^5D_0 \rightarrow {}^7F_1$ (580-600 nm) calculated by formula (1), depends on the symmetry of the Eu^{3+} environment. This value is called the degree of asymmetry of the Eu^{3+} ion environment. It is known that the higher the value of *R*, the more attractive the material is as a red phosphor:

$$R = \frac{I(^5D_0 \rightarrow {}^7F_2)}{I(^5D_0 \rightarrow {}^7F_1)}. \quad (1)$$

The *R* values calculated from spectra 1 and 2 in Figure 2 are 1.63 and 1.77, respectively. They are significantly lower than the value of $R \approx 2.7$ for Eu^{3+} ions at the C_{2v} symmetry position (Bettinelli *et al.*, 1996). This difference between the data obtained can be explained by the presence of emission bands of Tb^{3+} ions ($^5D_4 \rightarrow {}^7F_4$ transitions) in the 580-600 nm region, which increases the value of the denominator in formula (1).

The photoluminescence intensity of the suspensions under xenon lamp excitation was insufficient to record the PL excitation spectra. Therefore, the excitation spectra were recorded only for the powder $K_3Tb_{0.9}Eu_{0.1}(PO_4)_2$ and NC films and composites "NC+$K_3Tb_{0.9}Eu_{0.1}(PO_4)_2$" (Fig. 3).

The red photoluminescence of the oxide, which is associated with the emission of Eu^{3+} ions, is effectively excited in the UV region of the spectrum (spectrum 1 in Fig. 3). Spectrum 2 excitation of the green PL of the powder $K_3Tb_{0.9}Eu_{0.1}(PO_4)_2$, associated with the emission of ions Tb^{3+}, is similar to spectrum 1, except for the band at 395 nm. It can be argued that in this oxide, an effective transfer of excitation energy from terbium to europium is realised, i.e., the sensitisation of the PL of Eu^{3+} ions by Tb^{3+} ions. The excitation energy transfer has been previously observed for other oxide materials containing this pair of ions (Xie *et al.*, 2015; Silveira *et al.*, 2020; Bu *et al.*, 2022). It should be noted that the excitation of red PL through the absorption of light by Tb^{3+} ions is more efficient than the direct excitation through the absorption of Eu^{3+} ions. Excitation of red luminescence of a composite film "NC+$K_3Tb_{0.9}Eu_{0.1}(PO_4)_2$" also occurs in the UV region due to the absorption of terbium and europium ions. The low-intensity luminescence of the nanocellulose film is excited in a multicomponent band lying in the spectral range of $\lambda < 480$ nm (spectrum 4 in Fig. 3).

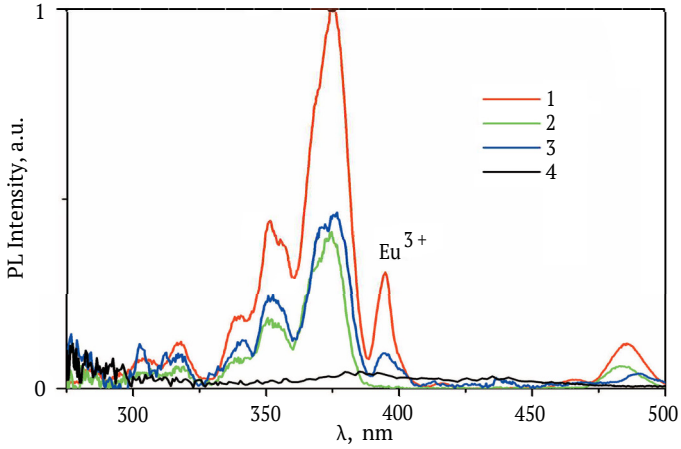

Figure 3. Photoluminescence excitation spectra

Note: powder $K_3Tb_{0.9}Eu_{0.1}(PO_4)_2$ (1, 2), film "NC+$K_3Tb_{0.9}Eu_{0.1}(PO_4)_2$" (3), NC film (4); registration at λ_{em}=618 (1, 3), 543 (2) and 570 nm (4), T=295 K

Source: compiled by the authors

Comparing the excitation spectra of the red PL (λ_{em}=618 nm) with the data obtained in the study by S. Kim *et al.* (2019) on the solar spectrum on the Earth's surface and the spectral efficiency of modern solar panels of various types, it is worth noting the following: at wavelengths shorter than 450 nm, silicon solar panels demonstrate less than 50% of their maximum efficiency, and at $\lambda < 380$ nm – less than 10%. At the same time, on the Earth's surface, the spectrum of solar radiation has a maximum in the 500 nm region but extends down to 300 nm. Accordingly, the shortwave part of solar radiation is used extremely inefficiently in the operation of solar panels. At the same time, such panels demonstrate the highest efficiency when illuminated in the 580-730 nm range, i.e., exactly where Eu^{3+} ions emit. Accordingly, the use of oxide $K_3Tb_{0.9}Eu_{0.1}(PO_4)_2$, in particular as components of a composite film "NC+$K_3Tb_{0.9}Eu_{0.1}(PO_4)_2$" as a fluorescent converter of UV radiation from the 330-400 nm range into red light, can increase the efficiency of solar panels (Bondar *et al.*, 2021).

Films "NC+$K_3Tb_{0,9}Eu_{0,1}(PO_4)_2$" can also be used as a coating to improve the efficiency of electricity-to-light converters – in LEDs. Among the cheapest LEDs are those that emit in the blue and UV spectral ranges. Figure 4 shows the UV spectra of composite films under laser excitation at 405 and 475 nm. The spectra differ both in the number and intensity of narrow europium emission lines and in the characteristics of the wide luminescence band of the cellulose matrix. That is, by changing the excitation wavelength, the colour of the coating can be controlled.

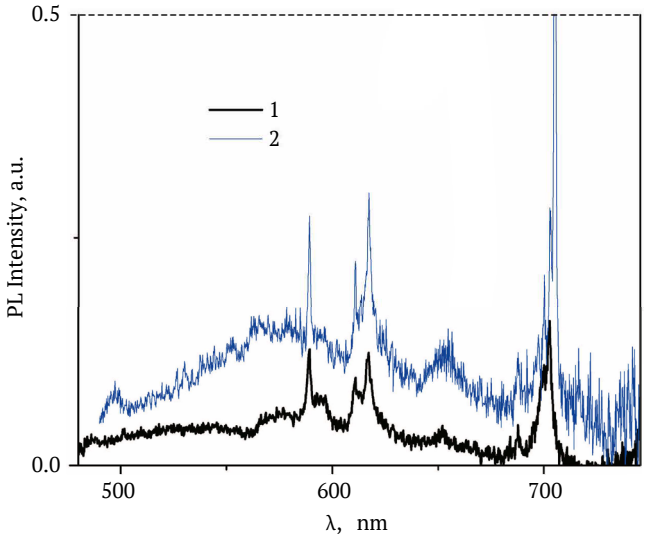

Figure 4. PL spectra of the "NC+$K_3Tb_{0.9}Eu_{0.1}(PO_4)_2$" films
Note: PL excitation at λ_{exc}=405 (1) and 473 nm (2), T=295 K
Source: compiled by the authors

Calculated *R*-values for PL of "NC+$K_3Tb_{0.9}Eu_{0.1}(PO_4)_2$" film under excitation at 405 and 473 nm are 1.95 and 3.25, respectively. A significant increase in *R* can be explained by the fact that the contribution of terbium luminescence in the 580-600 nm region decreases compared to europium luminescence. According to the results of C. Zuo *et al*. (2015), the PL excitation spectra of Tb^{3+} ions in the visible region show that at λ_{ex} = 405 nm these ions do not emit, and at λ_{exc} = 473 nm their low-intensity luminescence is possible. Thus, the results on the PL of the NC+$K_3Tb_{0.9}Eu_{0.1}(PO_4)_2$ films can be explained based on the literature data mentioned in this section on the peculiarities of the crystal structure of $M_3RE(PO_4)_2$ compounds and the luminescence of Eu^{3+} and Tb^{3+} ions in oxides.

To check the efficiency of UV light absorption and its conversion into visible radiation, the visible radiation spectra of an LED with λ_{max} = 375 nm and a test system based on the same LED with a "NC+$K_3Tb_{0.9}Eu_{0.1}(PO_4)_2$" film were recorded. The film was placed directly after the LED. V. Veleschuk *et al.* (2019) found that high-power UV LEDs have parasitic emission in the blue and yellow regions due to electroluminescence. Similar parasitic blue and yellow emission is observed for the used UV LED (spectrum 1 in Fig. 5).

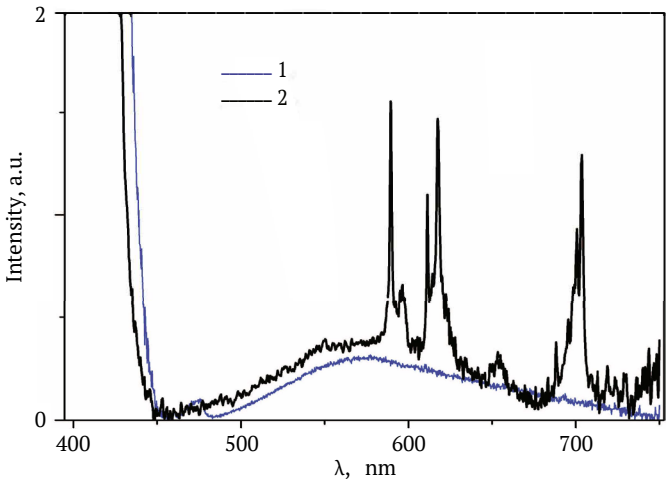

Figure 5. Radiation spectra
Note: 1 – UV LED (λ_{max}=375 nm); 2 – "UV LED + film "NC+$K_3Tb_{0,9}Eu_{0,1}(PO_4)_2$"; T=295 K
Source: compiled by the authors

In the case of the LED + film system, stray radiation is attenuated due to the low transparency of the film. At the same time, narrow emission lines of europium ions are observed. It can also be assumed that the broadband

with a maximum at 580 nm is a superposition of the diode electroluminescence band and the nanocellulose photoluminescence band. Colour coordinates are often used to assess the colour characteristics of radiation. The colour coordinates according to CIE 1931 (Schanda, 2007) for white are (x = 0.333; y = 0.333). The presence of luminescence in the blue and yellow spectral regions of the UV LED leads to colour coordinates corresponding to blue light (x = 0.214; y = 0.079). Adding a film "NC+$K_3Tb_{0.9}Eu_{0.1}(PO_4)_2$" leads to a shift in the coordinates to the red region (x = 0.304; y = 0.196). The coordinate offset on the chromaticity diagram for the CIE 1931 standard is shown in Figure 6.

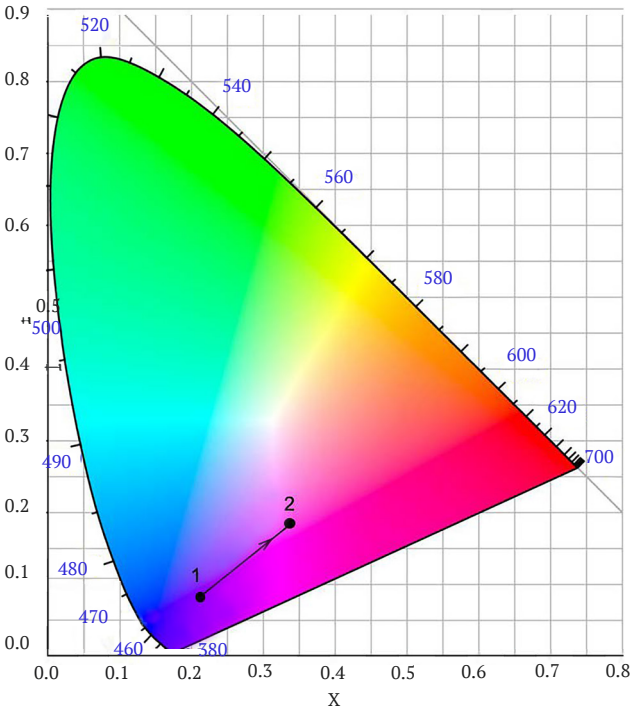

Figure 6. Position of the radiation colour coordinates on the chromaticity diagram

Note: 1 – UV LED (λ_{max}=375 нм); 2 – "UV LED + film "NC+$K_3Tb_{0.9}Eu_{0.1}(PO_4)_2$"; T=295 K

Source: compiled by the authors

Thus, the investigated composite films are promising luminescent LED coatings. The "red" shift of colour coordinates is insufficient, partially due to the small film thickness, which is only 90 ± 10μ m. It can be assumed that an increase in film thickness will lead to enhanced absorption of the blue radiation of the LED and better conversion of the absorbed energy into yellow and red radiation and, accordingly, to improvement of the colour characteristics of the radiation.

CONCLUSIONS

Samples of thin films based on nanocellulose and oxide were prepared by a simple evaporation method from aqueous suspensions. According to the results of optical microscopy, the films contained micro/nanoscale cellulose formations, such as crystals and fibrils. The largest oxide crystals $K_3Tb_{0.9}Eu_{0.1}(PO_4)_2$ had a size of about 300 μm. A fairly uniform distribution of oxide crystals with an average size of about 50 μm was observed in the composite films within the areas of ≈ 0.5 × 0.5 mm². The presence of water molecules, which is manifested in their Raman scattering lines, probably causes the low luminescence intensity of the studied suspensions.

Intense red photoluminescence of the powder $K_3Tb_{0.9}Eu_{0.1}(PO_4)_2$ and thin film "nanocellulose+$K_3Tb_{0.9}Eu_{0.1}(PO_4)_2$", associated with the emission of Eu^{3+} ions, is effectively excited by absorption by terbium ions in the region of 330-400 nm. This is evidence of the efficient transfer of excitation energy from Tb^{3+} ions to Eu^{3+} ions. The presence of red luminescence excitation in the region of 330-400 nm is important from the point of view of developing luminescent converters for solar panels based on the studied films.

Values of the degree of asymmetry calculated from the emission spectra of the powder $K_3Tb_{0.9}Eu_{0.1}(PO_4)_2$, suspensions, and films "nanocellulose+$K_3Tb_{0.9}Eu_{0.1}(PO_4)_2$", is in the range of 1.63-3.25, indicating a low symmetry of the Eu^{3+} ion environment. The significant change in the degree of asymmetry with the excitation wavelength is attributed to the change in the contribution of Tb^{3+} ions to the overall photoluminescence spectrum in the 580-600 nm range.

Films "nanocellulose+$K_3Tb_{0.9}Eu_{0.1}(PO_4)_2$" are capable of absorbing ultraviolet LED radiation and transforming the absorbed energy into yellow and red light. Chromaticity coordinates of the ultraviolet LED with λ_{max}=375 nm equipped with a composite film shift towards the standard for white light.

The investigated materials have the potential to be used as luminescent converters in power generation and conversion devices such as solar panels and LEDs. Further research in this area will be aimed at optimising the concentration of europium ions in the oxide $K_3Tb_{1-x}Eu_x(PO_4)_2$, the ratio between the amount of oxide and nanocellulose, and the film thickness.

ACKNOWLEDGEMENTS

This research was funded by the Ministry of Education and Science of Ukraine. The authors are sincerely grateful to Professor V. A. Barbash (National Technical University of Ukraine "Igor Sikorsky Kyiv Polytechnic Institute") for providing nanocellulose suspensions for the study.

CONFLICT OF INTEREST

None.

REFERENCES

[1] Ahirwar, R., & Tripathi, A.K. (2021). E-waste management: A review of recycling process, environmental and occupational health hazards, and potential solutions. *Environmental Nanotechnology, Monitoring & Management*, 15, article number 100409. doi: 10.1016/j.enmm.2020.100409.

[2] Barbash, V.A., Yashchenko, O.V., & Vasylieva, O.A. (2019). Preparation and properties of nanocellulose from miscanthus x giganteus. *Journal of Nanomaterials*, *2019*, article number 3241968. doi: 10.1155/2019/3241968.
[3] Beran, A., Voll, D., & Schneider, H. (2001). Dehydration and structural development of mullite precursors: An FTIR spectroscopic study. *Journal of the European Ceramic Society*, 21(14), 2479-2485. doi: 10.1016/S0955-2219(01)00265-5.
[4] Bettinelli, M., Speghini, A., Ferrari, M., & Montagna, M. (1996). Spectroscopic investigation of zinc borate glasses doped with trivalent europium ions. *Journal of Non-Crystalline Solids*, 201(3), 211-221. doi: 10.1016/0022-3093(96)00134-2.
[5] Binnemans, K. (2009). Lanthanide-based luminescent hybrid materials. *Chemical Reviews*, 109(9), 4283-4374. doi: 10.1021/cr8003983.
[6] Bondar, I.I., Suran, V.V., Mynya, O.Y., Shuaibov, O.K., Shevera, I.V., & Krasilinets, V.M. (2021). Formation of structured films upon irradiation of an aqueous solution of copper sulphate with high-power laser radiatio. *Scientific Herald of Uzhhorod University. Series "Physics"*, 49, 43-47.
[7] Bu, X., Liu, Y.G., & Chen, J. (2022). Band structure, photoluminescent properties, and energy transfer behavior of a multicolor tunable phosphor $K_3Lu(PO_4)_2$: Tb^{3+},Eu^{3+} for warm white light-emitting diodes. *Journal of Luminescence*, 251, article number 119133. doi: 10.1016/j.jlumin.2022.119133.
[8] Choe, D., Kim, Y.M., Nam, J.E., Nam, K., Shin, C.S., & Roh, Y.H. (2018). Synthesis of high-strength microcrystalline cellulose hydrogel by viscosity adjustment. *Carbohydrate polymers*, 180, 231-237. doi: 10.1016/j.carbpol.2017.10.017.
[9] Choi, S.M., Rao, K.M., Zo, S.M., Shin, E.J., & Han, S.S. (2022). Bacterial cellulose and its applications. *Polymers*, 14(6), article number 1080. doi: 10.3390/polym14061080.
[10] Dorenbos, P. (2000). The $4f^n \leftrightarrow 4f^{n-1}5d$ transitions of the trivalent lanthanides in halogenides and chalcogenides. *Journal of Luminescence*, 91(1-2), 91-106. doi: 10.1016/S0022-2313(00)00197-6.
[11] Fang, Z., Zhang, H., Qiu, S., Kuang, Y., Zhou, J., Lan, Y., Sun, C., Li, G., Gong, S., & Ma, Z. (2021). Versatile wood cellulose for biodegradable electronics. *Advanced Materials Technologies*, 6(2), article number 2000928. doi: 10.1002/admt.202000928.
[12] Farmer, J.M., Boatner, L.A., Chakoumakos, B.C., Rawn, C.J., & Richardson, J. (2016). Structural and crystal chemical properties of alkali rare-earth double phosphates. *Journal of Alloys and Compounds*, 655, 253-265. doi: 10.1016/j.jallcom.2015.09.124.
[13] Forti, V., Baldé, C.P., Kuehr, R., & Bel, G. (2020). The global e-waste monitor 2020. Retrieved from https://ewastemonitor.info/wp-content/uploads/2020/11/GEM_2020_def_july1_low.pdf.
[14] Gan, J., Wu, Y., Yang, F., Zhang, H., Wu, X., Wang, Y., & Xu, R. (2022). Wood-cellulose photoluminescence material based on carbon quantum dot for light conversion. *Carbohydrate Polymers*, 290, article number 119429. doi: 10.1016/j.carbpol.2022.119429.
[15] Gemeda, G.F., Etefa, H.F., Hsieh, C.C., Kebede, M.A., Imae, T., & Yen, Y.W. (2022). Preparation of ZnO/NiO-loaded flexible cellulose nanofiber film electrodes and their application to dye-sensitized solar cells. *Carbohydrate Polymer Technologies and Applications*, 3, article number 100213. doi: 10.1016/j.carpta.2022.100213.
[16] Indriyati, I., Irmawati, Y., & Puspitasari, T. (2019). Comparative study of bacterial cellulose film dried using microwave and air convection heating. *Journal of Engineering and Technological Sciences*, 51(1), 121-132. doi: 10.5614/j.eng.technol.sci.2019.51.1.8.
[17] Kim, S., Jahandar, M., Jeong, J.H., & Lim, D.C. (2019). Recent progress in solar cell technology for low-light indoor applications. *Current Alternative Energy*, 3(1), 3-17. doi: 10.2174/1570180816666190112141857.
[18] Liu, X., Huang, K., Lin, X., Li, H., Tao, T., Wu, Q., Zheng, Q., Huang, L., Ni, Y., Chen, L., Ouyang, X., & Li, J. (2020). Transparent and conductive cellulose film by controllably growing aluminum doped zinc oxide on regenerated cellulose film. *Cellulose*, 27, 4847-4855. doi: 10.1007/s10570-020-03147-0.
[19] Mikhailik, V.B., Kraus, H., & Dorenbos, P. (2009). Efficient VUV sensitization of Eu^{3+} emission by Tb^{3+} in potassium rare-earth double phosphate. *Physica Status Solidi (RRL)–Rapid Research Letters*, 3(1), 13-15. doi: 10.1002/pssr.200802211.
[20] Nedielko, M., Hamamda, S., Alekseev, O., Chornii, V., Dashevskii, M., Lazarenko, M., Kovalov, K., Nedilko, S.G., Tkachov, S., Revo, S., & Scherbatskyi, V. (2017). Mechanical, dielectric, and spectroscopic characteristics of "micro/nanocellulose+ oxide" composites. *Nanoscale Research Letters*, 12(1), article number 98. doi: 10.1186%2Fs11671-017-1862-x.
[21] Nedielko, M., Alekseev, O., Chornii, V., Kovalov, K., Lazarenko, M., Nedilko, S., Scherbatskyi, V., Boyko, V., & Sheludko, V. (2018). Structure and properties of microcrystalline cellulose "Ceramics-Like" composites incorporated with $LaVO_4$:Sm oxide compound. *Acta Physica Polonica A*, 133(4), 838-842. doi: 10.12693/APhysPolA.133.838.
[22] Pal, B., Matsoso, J.B., Parameswaran, A.K., Roy, P.K., Lukas, D., Luxa, J., Marvan, P., Azadmanjiri, J., Hrdlicka, Z., Jose, R., & Sofer, Z. (2022). Flexible, ultralight, and high-energy density electrochemical capacitors using sustainable materials. *Electrochimica Acta*, 415, article number 140239. doi: 10.1016/j.electacta.2022.140239.
[23] Raut, N.C., & Al-Shamery, K. (2018). Inkjet printing metals on flexible materials for plastic and paper electronics. *Journal of Materials Chemistry C*, 6, 1618-1641. doi: 10.1039/C7TC04804A.

[24] Reisfeld, R., Zigansky, E., & Gaft, M. (2004). Europium probe for estimation of site symmetry in glass films, glasses and crystals. *Molecular Physics*, 102(11-12), 1319-1330. doi: 10.1080/00268970410001728609.
[25] Schanda, J. (Ed.). (2007). *Colorimetry: Understanding the CIE system*. New Jersey: John Wiley & Sons.
[26] Silveira, W.S., Nascimento, P.A., Silva, A.J., & Rezende, M.V.D.S. (2020). Luminescent properties and energy transfer mechanism from Tb^{3+} to Eu^{3+} doped in $Y_3Al_5O_{12}$ phosphors. *Journal of Alloys and Compounds*, 822, article number 153651. doi: 10.1016/j.jallcom.2020.153651.
[27] Terebilenko, K.V., Bychkov, K.L., Klymyshyna, K.E., Baumer, V.N., Slobodyanik, M.S., Khomenko, E.V., & Dotsenko, V.P. (2017). Single crystals of $KRE(MoO_4)_2$, (RE-Ce, Pr) obtained from fluorides: scheelite-related structure and luminescence. *Crystal Research and Technology*, 52(12), article number 1700222. doi: 10.1002/crat.201700222.
[28] Urbina, L., Corcuera, M.Á., Gabilondo, N., Eceiza, A., & Retegi, A. (2021). A review of bacterial cellulose: sustainable production from agricultural waste and applications in various fields. *Cellulose*, 28(13), 8229-8253. doi: 10.1007/s10570-021-04020-4.
[29] Veleschuk, V., Vlasenko, A., Vlasenko, Z., Petrenko, I., Malyi, Y., Borshch, V., Borshch, O., & Shefer, A. (2019). Current-voltage characteristic and electroluminescence of UV LEDs 365 nm at liquid nitrogen temperature. *Optica Applicata*, 49(1), 125-133. doi: 10.5277/oa190111.
[30] Wang, Q., Sun, J., Yao, Q., Ji, C., Liu, J., & Zhu, Q. (2018). 3D printing with cellulose materials. *Cellulose*, 25, 4275-4301. doi: 10.1007/s10570-018-1888-y.
[31] Wang, P., Yin, Y., Fang, L., He, J., Wang, Y., Cai, H., Yang, Q., Shi, Z., & Xiong, C. (2023). Flexible cellulose/PVDF composite films with improved breakdown strength and energy density for dielectric capacitors. *Composites Part A: Applied Science and Manufacturing*, 164, article number 107325. doi: 10.1016/j.compositesa.2022.107325.
[32] Xie, F., Li, J., Dong, Z., Wen, D., Shi, J., Yan, J., & Wu, M. (2015). Energy transfer and luminescent properties of $Ca_8MgLu(PO_4)_7$: Tb^{3+}/Eu^{3+} as a green-to-red color tunable phosphor under NUV excitation. *RSC Advances*, 5(74), 59830-59836. doi: 10.1039/C5RA08680A.
[33] Zhao, D., Zhu, Y., Cheng, W., Chen, W., Wu, Y., & Yu, H. (2021). Cellulose-based flexible functional materials for emerging intelligent electronics. *Advanced materials*, 33(28), article number 2000619. doi: 10.1002/adma.202000619.
[34] Zhu, X., Jiang, G., Wang, G., Zhu, Y., Cheng, W., Zeng, S., Zhou, J., Xu, G., & Zhao, D. (2023). Cellulose-based functional gels and applications in flexible supercapacitors. *Resources Chemicals and Materials*, 2(2), 177-188. doi: 10.1016/j.recm.2023.03.004.
[35] Zhuravlov, O.Yu., Shyian, O.V., Shirokov, B.M., Kolodiy, I.V., & Sholohov, S.M. (2021). Sublimation process for obtaining silicon films from molybdenum and tungsten disilicide. *Scientific Herald of Uzhhorod University. Series "Physics"*, 49, 48-53.
[36] Zou, C., Qu, D., Jiang, H., Lu, D., Ma, X., Zhao, Z., & Xu, Y. (2019). Bacterial cellulose: A versatile chiral host for circularly polarized luminescence. *Molecules*, 24(6), article number 1008. doi: 10.3390/molecules24061008.
[37] Zuo, C., Zhou, Z., Zhu, L., Xiao, A., Chen, Y., Zhang, X., Zhuang, Y., Li, X., & Ge, Q. (2015). Luminescence properties of Tb^{3+}-doped borosilicate scintillating glass under UV excitation. *Spectrochimica Acta Part A: Molecular and Biomolecular Spectroscopy*, 147, 324-327. doi: 10.1016/j.saa.2015.03.097.

Володимир Васильович Бойко
Кандидат фізико-математичних наук, доцент
Національний університет біоресурсів і природокористування України
03041, вул. Героїв Оборони, 15, м. Київ, Україна
https://orcid.org/0000-0003-2926-2752
Віталій Петрович Чорній
Кандидат фізико-математичних наук
Національний університет біоресурсів і природокористування України
03041, вул. Героїв Оборони, 15, м. Київ, Україна
https://orcid.org/0000-0003-3727-5617
Сергій Герасимович Неділько
Доктор фізико-математичних наук, старший науковий співробітник
Київський національний університет імені Тараса Шевченка
01601, вул. Володимирська, 64/13, м. Київ, Україна
https://orcid.org/0000-0001-5196-6807
Катерина Володимирівна Теребіленко
Доктор хімічних наук, доцент
Київський національний університет імені Тараса Шевченка
01601, вул. Володимирська, 64/13, м. Київ, Україна
https://orcid.org/0000-0003-2403-4347

Люмінесцентні конвертери на основі композитних плівок «наноцелюлоза + $K_3Tb(PO_4)_2$:Eu»

Анотація. Перевагами целюлози та її похідних, як новітніх матеріалів для пристроїв, що виробляють, накопичують та перетворюють електроенергію є їх дешивизна, екологічність, легкість утилізації та можливість виготовлення різними способами і з різної сировини, в тому числі, і з відходів агропромисловості. Саме тому їх дослідження як матеріалів для сучасної техніки та електроніки є актуальним. Метою цієї роботи було з'ясування люмінесцентних характеристик композиційних плівок, виготовлених на основі наноцелюлози та полікристалічного оксиду $K_3Tb_{0,9}Eu_{0,1}(PO_4)_2$. Оптична мікроскопія та спектрально-люмінесцентний метод були застосовані для характеризації виготовлених плівок та їх вихідних компонент. З'ясовано, що кристаліти з середнім розміром близько 50 μм розподілені досить рівномірно у плівці «наноцелюлоза+$K_3Tb_{0,9}Eu_{0,1}(PO_4)_2$». Для досліджених зразків у формі суспензій спостерігалась смуга Раманівського розсіяння світла з максимумом на 564 нм при лазерному збудженні на 473 нм. Інтенсивність фотолюмінесценції наноцелюлози у вигляді суспензії та в плівках є низькою в порівнянні зі свіченням оксиду як наповнювача. Свічення іонів Eu^{3+} є інтенсивним в червоній області спектра. Обчислені значення ступеня асиметричності вказують на низьку симетрію позицій, які займають іони європію в оксиді та на внесок випромінювання іонів Tb^{3+} в загальний спектр композитної плівки. За результатами досліджень з'ясовано, що люмінесценцію іонів Eu^{3+} сенсибілізовано іонами Tb^{3+}, які поглинають збуджуюче світло з подальшою передачею енергії до іонів європію. Положення смуг поглинання іонів Eu^{3+} та Tb^{3+} в ультрафіолетовій ділянці спектра та інтенсивне випромінювання Eu^{3+} в червоній області вказують на перспективність використання плівок «наноцелюлоза+ $K_3Tb_{0,9}Eu_{0,1}(PO_4)_2$» для підвищення ефективності сонячних панелей. Тестування плівок при збудженні люмінесценції ультрафіолетовим випромінюванням світлодіоду ($\lambda_{зб}$ = 375 нм) показало можливість розробки на їх основі білих світлодіодів. Зокрема, координати колірності світлодіода без покриття становили (x = 0,214; y = 0,079), а використання плівки – композиту, як покриття, призводить до зміщення координат до червоної області: x = 0,304, y = 0,196. Одержані результати щодо морфології та люмінесцентних властивостей можуть бути використані для оптимізації складу та умов виготовлення композитних плівок типу «наноцелюлоза+$K_3Tb_{0,9}Eu_{0,1}(PO_4)_2$» для їх застосування як люмінесцентних конвертерів у світлодіодах або сонячних панелях

Ключові слова: іон; сенсибілізація; світлодіод; сонячна панель; фотолюмінесценція; покриття